Scientific Research Publishing

Journal of Computer and Communications, 2022, 10, 103-112
https://www.scirp.org/journal/jcc
ISSN Online: 2327-5227
ISSN Print: 2327-5219

A Control Method for SMA Robotic Actuators

Tian Lyu

School of Mechatronics Engineering, Beijing Institute of Technology, Beijing, China
Email: jasonlvernexlzy@hotmail.com

How to cite this paper: Lyu, T. (2022) A Control Method for SMA Robotic Actuators. *Journal of Computer and Communications*, **10**, 103-112.
https://doi.org/10.4236/jcc.2022.105007

Received: April 6, 2022
Accepted: May 28, 2022
Published: May 31, 2022

Abstract

Soft robots show remarkable benefits over conventional rigid robots due to their high energy density and other factors. We propose a circular soft robot integrating the control system, actuating it with several shape memory alloy (SMA) actuators. Our research methodology involved connecting the DC voltage supply and L298N module to provide uninterrupted power to the actuator and thence control the actuator via Arduino Uno MCU and TOF camera. We designed the controller to simultaneously complete the positioning and manipulation tasks. A novel method utilizing visual servo and closed-loop control algorithm was proposed and integrated into the controller. This method involves the implementation of multi-gait locomotion using SMA actuators. Additionally, the development of closed-loop dynamic controllers for a continuous soft robot is also evaluated. The proposed control model is designed and simulated on the MATLAB tool. To verify the efficiency of the proposed forward-feedback controller, simulations and experiments were conducted in the current study. A new control method using PID control based on the Kalman filtering algorithm and visual servo for the SMA actuator designed in this research is introduced. We conclude that applying spike excitation voltage would benefit the actuating performance. Overall, the experimental results demonstrated a promising future for the purposed control method.

Keywords

Soft Robotics, Shape Memory Alloys, Visual Servo, PID Control

1. Introduction

Besides rigid robotics, soft robotics has shown greater efficiency in adapting to complex environments [1] [2] [3]. As soft robotics could be regarded as a complex rigid robot with infinite joints [4], it revealed a lack of appropriate control strategies, thus creating obstacles to the precise control of soft robotics [5].

Shape Memory Alloys (SMAs), as one of the novel materials, though found suitable for actuators of soft robotics, have a limitation of being short of control strategies [1] [2] [3] [6].

Fei *et al.* proposed a closed-loop control method embedding four curvature sensors as the feedback signals [1] [3]. However, their strategy involved a meticulous forging of the steel shell and affixing of the sensors, which increases the complexity of the system and scale. Cheng *et al.* developed an SMA-based soft robot, with a motion processing unit (MPU) for sending back the angular and velocity data [2]. Nevertheless, control methods based on integrated sensor feedback are feasible to operate larger-scale robots but not the centimetre-scale robot in this study. Consequently, a suitable control strategy for centimeter-scale soft robots is required. More measures can be found in controlling soft robots. Fan *et al.* applied Visual Servo to a type of soft robot and concluded this method's active regulation as being more efficient [7]. Instead of attaching peripheral sensors to the small-scale soft robots, the method of using a camera set to capture the position changes of the coiled robots should be considered. Nuchkrua T *et al.* proposed a contouring control of the robot, focusing on the error of the robot's end-factor [8]. This could be achieved by detecting the end terminals of the actuators via computer vision. Hence, it was implemented in the current research.

Therefore, a control system with a visual servo as the input signal and an integrated Proportional Integral Derivative (PID) and Kalman filter as the control algorithm is proposed.

This study aims to develop a control strategy. The rest of this paper is organized as follows: In Section 2, a control model is designed and simulated on the MATLAB tool. In Section 3, the setup of the prototype and experiments is demonstrated. In Section 4, conclusions and expectations from this research are presented.

2. Design and Simulation of the Control System

This control system aims to achieve the maximum position that an actuator can reach. Since the soft robot designed in this research gains mobility by extending its actuators to acquire friction force and reaction force, the position or deformation control of the actuators enables accurate control of this centimeter-scale robot.

To better simulate or construct a control system, a sufficient amount of data was obtained by recording the performance of a single actuator under different parameters. It showed the relationship among the diameter of the SMA coil wire, excitation voltage to generate the deformation of the SMAs, pulse width for excitation, pulse width for restoration, length of SMA coils, etc.

An optimized selection of the parameters is chosen. By altering its excitation pulse width duration, the maximum position of the actuator could be controlled. Afterward, a scattered map in relation to maximum deformation and excitation

time is drawn using the data obtained. The Fourier fitting method is applied to obtain the input-output curve of the system [9].

Hence, the function of the curve can be determined using the following Equation (1):

$$O(t) = 37.31 - 8.766\cos(0.0427t) - 1.84\sin(0.0427t) \tag{1}$$

where, $O(t)$ denotes the deformation function of the actuator and signifies the duration of the excitation pulse. The graph shows a partial nonlinearity since its nonlinearity happens only in extreme conditions when excitation time is either too short or long. So, in a general control, we could still apply traditional control methods to this slightly nonlinear system.

Using Equation (1), we can obtain the transfer function in the frequency domain of the control system as:

$$TF(s) = \frac{133}{s^2 + 25s} \tag{2}$$

PID is commonly used in various linear control situations due to the deviation of the initial state and the uncertainty of the model, appropriately induced noise is conducive to a faster approximation to the real state. During the control process, noises or bias can be induced by several factors like manual measurement error, camera measurement error, etc. So, a PID control based on the Kalman filtering algorithm is suitable for the filtration of the controlled noise and the measuring noise [10].

Figure 1 shows the block diagram of the PID control based on the Kalman filtering algorithm control system. By cascading the two major control algorithms, we can obtain the following Equations (3-6):

From PID control [11], we can obtain:

$$u = k_p\left[e(t) + k_i\int_0^t e(t)\mathrm{d}t + k_d\frac{\mathrm{d}e(t)}{\mathrm{d}t}\right] \tag{3}$$

where, u is the output of the PID block.

From the Kalman filter, we have:

$$x_{k+1} = Ax_k + Bu_k \tag{4}$$

$$P_{k+1} = AP_kA^{\mathrm{T}} + Q \tag{5}$$

$$K_k = P_kH^{\mathrm{T}}\left(HP_kH^{\mathrm{T}} + R\right)^{-1} \tag{6}$$

$$x_k = x_k + K_k\left(z_k - Hx_k\right) \tag{7}$$

$$P_k = \left(I - K_kH\right)P_k \tag{8}$$

where, R and Q indicate the control error and measured error, respectively, in the diagram. Further, P_k denotes the anticipated actual position at present.

For y_d in diagram 2, we can predefine the demanded gait for the actuator. y in the diagram shows the data received from the camera and y_e is the anticipated actual gait same as the output value of Equation (8).

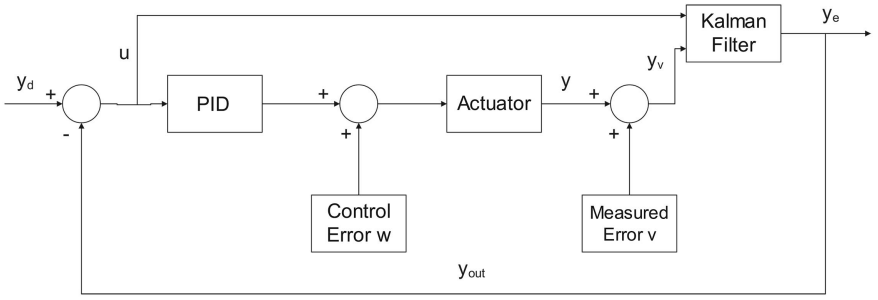

Figure 1. PID control based on the Kalman filtering algorithm block.

Accordingly, we can simulate the control process of the system via MATLAB software. The demanded gait was set to a constant 20 mm, and random noise was set to generate within a range of 1.

R, Q, k_p, k_I, k_D rely more on practical usage conditions, so in the simulation, they are set to be the value that does not affect the evaluation of this method and is calibrated in the actual experiment.

Table 1 shows the inputs variables and their values. As listed in the table, where a and b stands for the coefficients in the transfer function. y_d is the demanded gait length, which remains constant of 200 during the simulation. M is the number of steps of the simulation, which is 3000 steps in this case. R, Q are variables used in the Kalman filtering process.

In Figure 2, the simulation result is plotted, where the red curve indicates the ideal output gait after PID, the black line shows the signal under noise conditions, and the blue line demonstrates the demanded gait. The plot shows that the method is deemed plausible due to a gradual constraining of the simulated output signal to the demanded signal.

Till now, the design and simulation process has been briefly described. The following section focuses on experiment setups and approaches.

3. Experiment

To modulate the pulse width of the excitation pulse, Microcontroller Units (MCUs) are adequate for this task. Yet, the principle of SMAs to deform is contingent on the electric power it receives as springs are electrified and heat is generated [1] [6]. The MCUs could not provide such large electric power to generate heat on the SMA wires so a DC voltage supply and an L298N module are needed.

The MCU used in this experiment is an Arduino Uno due to its simplicity. The DC voltage supply and L298N module are connected, as shown in Figure 3. Thus, sufficient and constant power can be directly supplied to the actuator.

Table 1. Inputs of the MATLAB simulation.

Item	a	b	M	y_d	Q	R
Value	25	133	3000	200	1	1

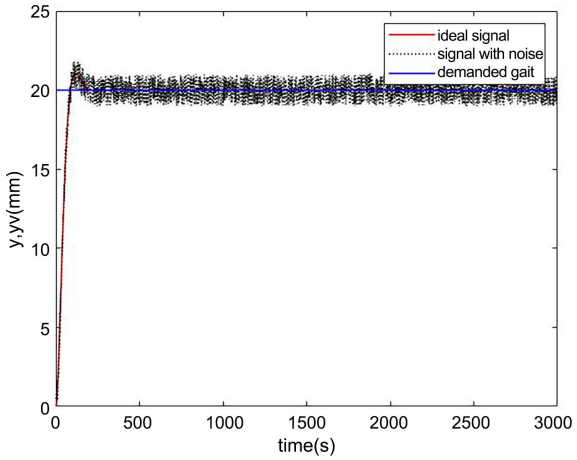

Figure 2. Result of the simulation.

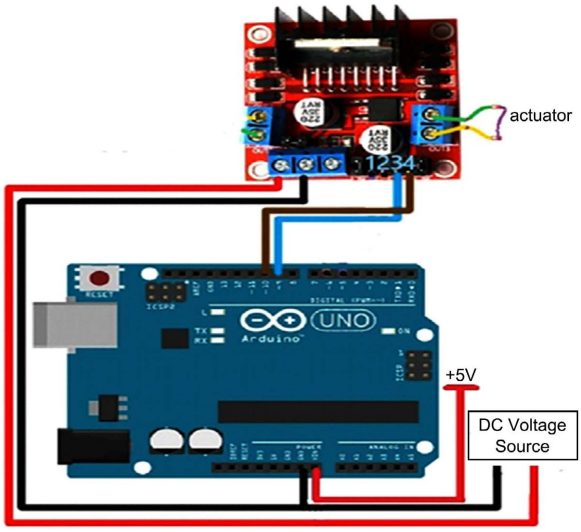

Figure 3. Hardware connection.

Figure 4 demonstrates a functional flow chart of MCU. The left part regarding receiving visual servo data from the computer is completed with a function block that is similar to a Universal Asynchronous Receiver-Transmitter (UART) interrupt. The UART block examines each package it receives from the computer and forsakes the invalid formatted packages. Maximum data are sorted and stored as a static variable in an appropriate package. This UART process is solitary from the main loop, thereby maintaining an optimal sampling rate despite the influence of the time delay function in the main loop. The maximum value is reset after the execution of the restoration process.

The visual servo in this experiment is aimed at detecting the distance between two marked points on the SMA wire and feedback on the real-time value.

A Time-of-Flight (TOF) camera (Axon Technology) is chosen. The M5 type camera has a detection range of 30 - 50 cm with 1 mm precision.

TOF camera has some advantages over other depth cameras such as binocular cameras and RGB depth cameras; it maintains unaffected or slightly affected

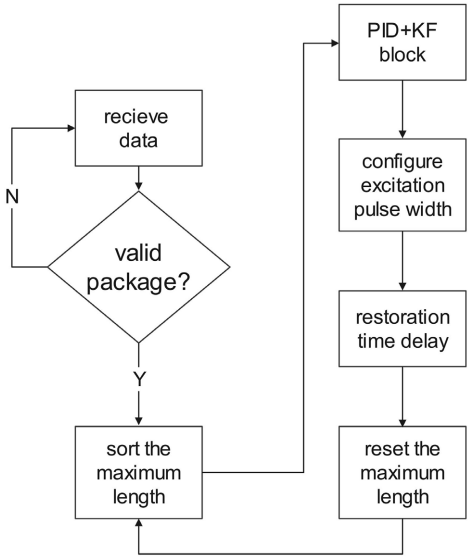

Figure 4. Functional flow chart of MCU.

under various lighting conditions. Yet, a TOF camera can achieve only a 30 fps frame rate, leading to loss of data when tracking high-speed motion. Nevertheless, this type of depth camera still fits this experiment because the restoring procedure of the SMA wires is relatively slow though excitation occurs in milliseconds. The samples just after the excitation of SMAs can be regarded as the maximum deformation.

Two orange play dough points are affixed to each end of the actuator. The mark points ought to be reduced to their minimum size to optimize the detection performance. To obtain the distance between the points of interest, two main procedures are included, namely clarifying the image to detect the points and calculating the world coordinates of the points.

In the first part of the procedure, each frame of the video's color stream is taken and converted to Hue Saturation Value (HSV) stream. The threshold value of the mark points is selected in the HSV frame and thence to crop the area of interest placing two mark points at the center. The cropping process is relatively inevitable since environmental color may contaminate the mark points' location approximation. Image dilation followed by contour retrieval is executed. Then, the geometric centers of the contours are determined.

Then, the coordinates of the centers could be conducted; the z coordinates of the centers can be obtained by mapping the depth stream and color stream, whereas the x and y positions could be converted from the image pixel coordinates after camera calibration (Qing) [12]. Still, only relative values are produced after these steps, so a precise gauge to measure the actual interval between the mark points is needed, in order to conduct the coefficient for each axis from image world coordinates to actual length separately. A general control system schematic diagram is shown in **Figure 5**.

The coordinates' data of the SMA actuator are sampled, calculated, and con-

verted to the approximate length on a laptop simultaneously. Meanwhile, the measured data from the visual servo along with demanded gait data, which can be pre-loaded on the MCU, are assigned to PID control based on the Kalman filtering algorithm. Eventually, a control signal is produced by MCU and the SMA robot is actuated.

Figure 6 demonstrates a general view of the test setups. The SMA actuator at one end is fixed on the white background with the other end free. Both terminals of the actuator are coated with white covers, and this is to eliminate the visual recognition error induced by the reflection of soldering material at the terminals of the SMA. Then, the SMA actuator is wired to the L298N module and the MCU.

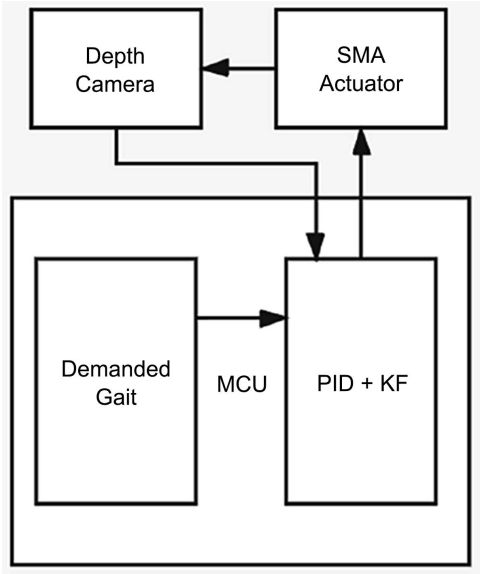

Figure 5. General control system scheme diagram.

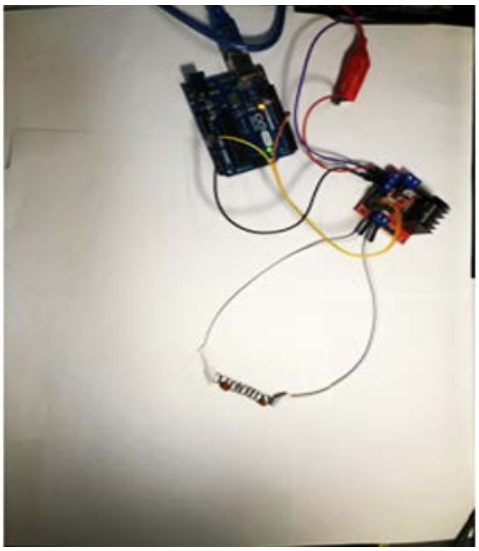

Figure 6. An overall view of an SMA actuator and its control system.

Actuating and controlling the SMA actuator in two conditions are tested; relatively low excitation voltage with more lasting pulse duration along with relatively high voltage with spike pulse excitation groups are recorded. By defining spike and gradual excitation, the excitation voltage lasting < 800 ms would be considered as a spike pulse, while 800 ms < voltage lasting < 4 s is considered as gradual excitation. Due to protecting the SMA wire from burning out, a upper limit of 4s excitation duration is selected. R, Q, k_p, k_I, k_D Parameters of PID control based on the Kalman filtering algorithm are carefully calibrated before data recording.

Lower excitation voltage requires a longer time for SMA to accumulate a sufficient amount of heat to deform, resulting in gradual distortion. This process is slow and conspicuous that the sampling rate of the TOF camera could fit the deformation procedure. To make the conjecture cogent, each test group uses different SMA actuators but is made to the approximately similar original length of 44 mm. Two groups of tests records are scattered in Figure 7(a). Both the test results show that the final maximum length has fallen into the margin of demand. The margin of demand is coded into MCU, defining 0.5 mm as its value, since the precision of the camera is 1 mm. On test 1, a gradual convergence can be seen according to the curve while on test 2, a maximum length regression of meeting the upper boundary of the range can be observed.

After several repetitions, our research proposes that applying spike excitation voltage would benefit the actuating performance. Such that a test sample of SMA actuator with an original length of 42 mm and demanded gait of 45 mm is plotted in Figure 7(b). The intercepted final convergence shows a satisfying result. Even though rapid deformation leads to the loss of sampling points on the excitation edge of the curve, the maximum length of the actuator still converges to set the target value.

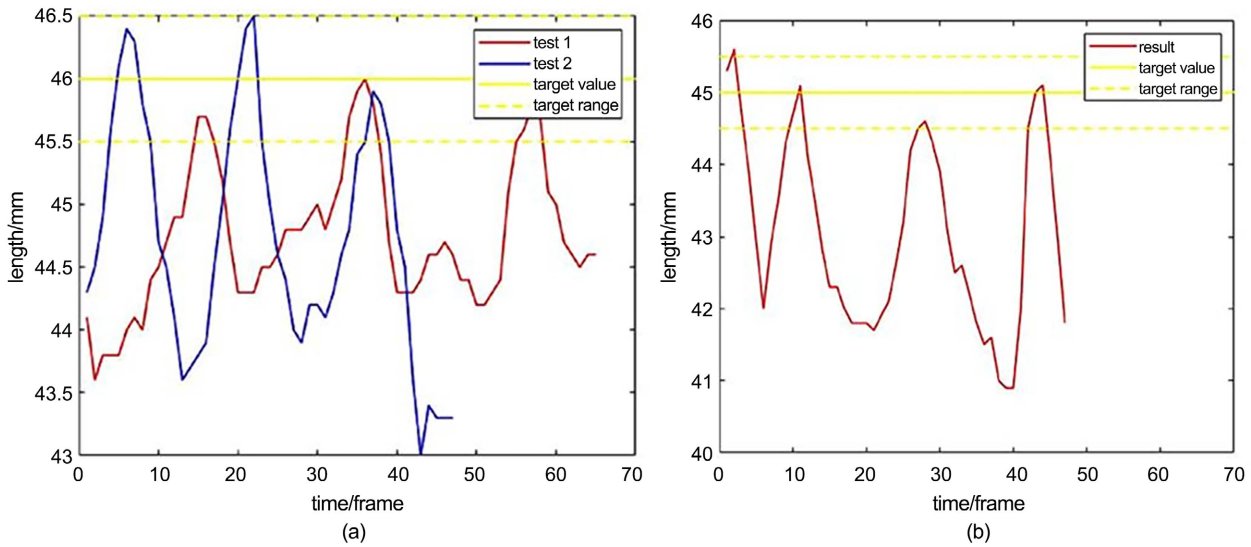

Figure 7. (a) Test data of gradual excitation, (Only final convergence interval intercepted), original length average: 44 mm targeted length: 46 0.5 mm; (b) Test data of spike excitation, (Only final convergence interval intercepted), original length average: 42 mm targeted length: 45 0.5 mm.

4. Conclusions

In this study, a control method using PID control based on the Kalman filtering algorithm and visual servo for the SMA actuator designed was introduced. Simulations with MATLAB and experiments are conducted, promising a prospecting future for the integral SMA soft robot and its control system.

Visual recognition stability and measurement precision are still technical barriers in this research. In future studies, we would embed a Reinforce Learning control of gait to this robotics system.

Data Availability

The raw/processed data required to reproduce these findings are available online at
https://github.com/JasonLvernex/PID-KALMAN-control-for-a-SMA-soft-robot-based-on-computer-vision

Conflicts of Interest

The author declares no conflicts of interest regarding the publication of this paper.

References

[1] Fei, Y. and Xu, H. (2017) Modeling and Motion Control of a Soft Robot. *IEEE Industrial Electronics Society— Transactions on Industrial Electronics*, **64**, 1737-1742. https://doi.org/10.1109/TIE.2016.2572670

[2] Cheng, C., Cheng, J. and Huang, W. (2019) Design and Development of a Novel SMA Actuated Multi-DOF Soft Robot. *IEEE Access*, **7**, 75073-75080. https://doi.org/10.1109/ACCESS.2019.2920632

[3] Li, J., Wang, J. and Fei, Y. (2019) Nonlinear Modeling on a SMA Actuated Circular Soft Robot with Closed-Loop Control System. *Nonlinear Dynamics*, **96**, 2627-2635. https://doi.org/10.1007/s11071-019-04949-z

[4] Wang, W.B., Xi, F.F., Tian, Y., Zhao, Y. and Li, Y. (2020) Modeling and Analysis of a Planar Soft Panel Continuum Mechanism. *Journal of Mechanisms and Robotics*, **12**, Article ID: 044503. https://doi.org/10.1115/1.4046029

[5] Della, S.C., Katzschmann, R.K., Bicchi, A. and Rus, D. (2020) Model-Based Dynamic Feedback Control of a Planar Soft Robot: Trajectory Tracking and Interaction with the Environment. *International Journal of Robotics Research*, **39**, 490-513. https://doi.org/10.1177/0278364919897292

[6] Mao, S., Dong, E., Jin, H., Xu, M., Zhang, S., Yang, J. and Low, K.H. (2014) Gait Study and Pattern Generation of a Starfish-Like Soft Robot with Flexible Rays Actuated by SMAs. *Journal of Bionic Engineering*, **11**, 400-411. https://doi.org/10.1016/S1672-6529(14)60053-6

[7] Xu, F., Wang, H., Liu, Z., Chen, W., and Wang, Y. (2021) Visual Servoing Pushing Control of the Soft Robot with Active Pushing Force Regulation. *Soft Robotics*. https://doi.org/10.1089/soro.2020.0178

[8] Nuchkrua, T. and Chen, S. (2016) Precision Contouring Control of Five Degree of Freedom Robot Manipulators with Uncertainty. *International Journal of Advanced Robotic Systems*, **2017**, 1-16. https://doi.org/10.1177/1729881416682703

[9] Ge, L., Chen J. and Li, R. (2017) Feedforward Control Based on Fourier Series Trajectory Fitting Method for Industrial Robot. 2017 29*th Chinese Control and Decision Conference* (*CCDC*), Chongqing, 28-30 May 2017, 4890-4894. https://doi.org/10.1109/CCDC.2017.7979361

[10] Hargrave, P.J. (1989) A Tutorial Introduction to Kalman Filtering. *IEE Colloquium on Kalman Filters*: *Introduction*, *Applications and Future Developments*, London, 21-21 February 1989, 1/1-1/6.

[11] IEE Colloquium on Getting the Best Out of PID in Machine Control (Ref. No.1996/287). *IEE Colloquium on Getting the Best Out of PID in Machine Control*, London, 24-24 October 1996.

[12] Qing (2019) Camera Calibration: Analysis of the Conversion Process from World Coordinate System to Image Pixel Coordinate System. https://blog.csdn.net/qq_27546529/article/details/89842373